Published in final edited form as:
Synapse. 2010 May ; 64(5): 350–362. doi:10.1002/syn.20734.

Striatal and extrastriatal dopamine release measured with PET and [^{18}F]fallypride

Mark Slifstein[1,2], **Lawrence S. Kegeles**[1,2], **Xiaoyan Xu**[1,2], **Judy L. Thompson**[1,2], **Nina Urban**[1,2], **John Castrillon**[1,2], **Elizabeth Hackett**[1,2], **Sung-A Bae**[1,2], **Marc Laruelle**[1,3], and **Anissa Abi-Dargham**[1,2]

[1]Columbia University

[2]New York State Psychiatric Institute

[3]GlaxoSmithKline

Abstract

The amphetamine challenge, in which PET or SPECT radioligand binding following administration of amphetamine is compared to baseline values, has been successfully used in a number of brain imaging studies as an indicator of dopaminergic function, particularly in the striatum. [^{18}F] fallypride is the first PET radioligand that allows measurement of the effects of amphetamine on D_2/D_3 ligand binding in striatum and extra-striatal brain regions in a single scanning session following amphetamine. We scanned 15 healthy volunteer subjects with [^{18}F] fallypride at baseline and following amphetamine (0.3 mg/kg) using arterial plasma input based modeling as well as reference region methods. We found that amphetamine effect was robustly detected in ventral striatum, globus pallidus and posterior putamen, and with slightly higher variability in other striatal subregions. However, the observed effect sizes in striatum were less than those observed in previous studies in our lab using [^{11}C] raclopride. Robust effect was also detected in limbic extra-striatal regions (hippocampus, amygdala) and substantia nigra, but the signal to noise ratio was too low to allow accurate measurement in cortical regions. We conclude that [^{18}F] fallypride is a suitable ligand for measuring amphetamine effect in striatum and limbic regions, but is not suitable for measuring the effect in cortical regions and may not provide the most powerful way to measure the effect in striatum.

Keywords

PET; positron emission tomography; amphetamine; dopamine; D2 receptors; schizophrenia

Introduction

The amphetamine challenge, in which PET or SPECT radioligand binding following administration of amphetamine is compared to baseline values, has been successfully used in a number of brain imaging studies as an indicator of dopaminergic function, particularly in the striatum. Studies have been published comparing the effects of amphetamine on radioligand binding to D2/3 receptors in various patient populations or have examined correlations between the magnitude of effect on binding of the radioligand with the subjective effects of the drug. The amphetamine paradigm has been used in studies of schizophrenia (Breier et al., 1997; Laruelle et al., 1999), schizotypal personality disorder (Abi-Dargham et al., 2004), alcohol dependence (Martinez et al., 2005; Munro et al., 2006a)

Correspondence: Mark Slifstein, PhD, 1051 Riverside Drive, Unit 31, New York NY 10032, 212 543 5872, mms218@columbia.edu.

and cocaine dependence (Martinez et al., 2004). The pharmacological effect, as measured with changes in radioligand binding has been correlated to performance on cognitive tasks (Aalto et al., 2005; Christian et al., 2006), subjective effects of the drug (Abi-Dargham et al., 1998; Drevets et al., 2001; Laruelle et al., 1995) effects of hormones and environmental stressors (Oswald et al., 2005; Oswald et al., 2007; Wand et al., 2007) and sex differences (Munro et al., 2006b; Riccardi et al., 2006b). Similar studies have been performed with other dopaminergic stimulants such as methylphenidate (Volkow et al., 1994). Most studies have been performed with radioligands that are antagonists at D_2/D_3 receptors, although some investigators have begun to explore the use of agonist tracers in amphetamine studies as well (Narendran et al., 2004; Willeit et al., 2008)

Radioligands that are specific to dopamine D2/3 receptors and have been used in this paradigm include the SPECT ligand [^{123}I] IBZM (Kung et al., 1989) ,the PET D2/D3 antagonists [^{11}C] raclopride (Ehrin et al., 1985), [^{11}C] NMSP (Dannals et al., 1984) , [^{18}F] FCP (Mach et al., 1996) , [^{18}F] fallypride (Mukherjee et al., 1996) [^{11}C] FLB 457 (Farde et al., 1997), and more recently, agonist radiotracers such as [^{11}C] NPA (Hwang et al., 2000), [^{11}C] MNPA (Finnema et al., 2005) and [^{11}C] PHNO (Wilson et al., 2005). Among the PET D2/3 antagonist radioligands, there are three that have been utilized in studies with human subjects and that have continued to appear in the recent amphetamine challenge literature. These are [^{11}C] raclopride, [^{11}C] FLB 457 and [^{18}F] fallypride. [^{11}C] raclopride has fast in vivo kinetics and moderate in vivo affinity, but because of its relatively low signal to noise ratio (affinity compared to nonspecific binding) the only brain region in which it can be used to reliably quantify receptor availability is the high receptor density striatum. Both [^{11}C] FLB 457 and [^{18}F] fallypride have higher affinity and signal-to-noise ratios in vivo and can provide reliable quantitative measures in extrastriatal brain regions where receptor density is an order of magnitude lower than in striatum. However, both ligands clear from the striatum much more slowly than [^{11}C] raclopride, such that washout from the striatum is too slow for quantitative imaging within the time constraints imposed by the rapid decay rate of ^{11}C. The maximal imaging time for obtaining adequate counts with ^{11}C is approximately 2 hrs and neither ligand reaches a washout phase in striatum by this time, a necessary condition for accurate quantitative measurement (Laruelle et al., 2003). Consequently, [^{11}C] FLB 457 can only be used for imaging extrastriatal regions. Because fallypride is labeled with ^{18}F, [^{18}F] fallypride scanning sessions can be extended for a longer duration than for ^{11}C labeled radioligands, so that it is possible to reliably quantify [^{18}F] fallypride binding in striatum. Thus [^{18}F] fallypride is unique in that it is the only currently available PET radiotracer than can simultaneously provide quantitative measures of D_2/D_3 receptor binding in the striatum and extrastriatal brain regions in the same scanning session. As most psychiatric disorders involve cortico-striatal circuits, imaging dopamine transmission simultaneously in striatal and extrastriatal regions would be a valuable tool if shown to be feasible and reliable. For this to be the case, [^{18}F] fallypride would have to prove to be equivalent to previously established tracers for striatal DA release (such as [^{11}C] raclopride) as well as reliable for extrastriatal regions that are of interest to the study of neuropsychiatric disorders, such as cortical and limbic regions.

In this study, we examined the amphetamine challenge in healthy volunteer subjects using [^{18}F] fallypride imaging to detect effects in striatal and extrastriatal regions in the same scanning session. Two other imaging groups have previously explored the amphetamine challenge using [^{18}F] fallypride in healthy volunteer subjects (Cropley et al., 2008; Riccardi et al., 2006a; Riccardi et al., 2006b). Those authors utilized orally administered amphetamine in different doses and did not obtain measurements of [^{18}F] fallypride concentration in arterial plasma. Cropley et al. (Cropley et al., 2008) scanned 14 healthy volunteers and measured test retest reproducibility, vulnerability to amphetamine challenge and vulnerability to dopamine depletion following α-MPT treatment. These authors reported

good reproducibility of baseline binding measures and detectable amphetamine effect in all striatal subregions and several extrastriatal regions (substantia nigra, medial and orbital prefrontal cortices) but were unable to detect an effect of dopamine depletion on [^{18}F] fallypride specific binding. Riccardi et al (Riccardi et al., 2006a) also examined 14 healthy control subjects and observed robust amphetamine effect in striatal subregions, temporal cortex, thalamus and substantia nigra, but did not examine pre-frontal cortex. In this study, we administered amphetamine at a dose of 0.3 mg/ kg i.v. and we measured arterial plasma activity in order to model data based on arterial input functions. Because neither of the previous [^{18}F] fallypride studies cited above utilized arterial input functions, it was not possible to ascertain whether changes in reference region distribution volume (cerebellum V_T) occurred across conditions and possibly contributed to or detracted from the observed effect following amphetamine. The acquisition of arterial plasma samples allowed us to estimate the non-displaceable distribution volume (V_{ND}) directly as cerebellum V_T, and to compare amphetamine effect measured with this more comprehensive approach to reference region analysis applied to the same data set. We also compared the amphetamine effect, as observed with [^{18}F] fallypride, to that which we previously reported with [^{11}C] raclopride (Martinez et al., 2003). The availability of historical data using the same dose and the same mode of administration of amphetamine (0.3 mg/kg i.v.), acquired on the same scanner and analyzed in the same laboratory allowed us to draw direct conclusions regarding the magnitude of striatal DA release measured with both tracers, and determine the extent to which [^{18}F] fallypride offers an advantage over a multiscan strategy using different tracers for different brain regions and requiring two administrations of amphetamine.

Methods

Subjects

Fifteen healthy human volunteers participated in the study (10 M, 5 F, age 25 ± 7 yrs). The study was approved by the Institutional Review Board of the New York State Psychiatric Institute. All subjects provided written informed consent. In each case, at the time of the PET scan, the absence of pregnancy, medical, neurological or psychiatric history was assessed by SCID-NP (including alcohol and drug abuse or current use of psychotropic medications) and by history, review of systems, physical examination, routine blood tests including pregnancy test, urine toxicology and EKG. Additionally, subjects underwent a high resolution T1 weighted MRI scan prior to participation in the PET study, which was assessed by a radiologist for any structural abnormalities that may preclude participation in the study.

Study design

Subjects were scanned on 2 separate days – once at baseline and once following amphetamine. Baseline scans were acquired first for each subject (interval between scans: 26 ± 31 days, range 2 to 121 days, or 19 ± 17 days, range 2 to 50 days with the 121 day subject removed). On the amphetamine day, subjects were intravenously injected with 0.3 mg/kg amphetamine over 45 s. Scanning commenced 30 min after amphetamine injection. In addition to arterial plasma samples taken to form an input function (See Arterial Input, below), plasma samples were drawn 10, 20 and 40 min after amphetamine injection (20 and 10 min before and 10 min after start of scan) for measurement of amphetamine levels.

PET acquisition and reconstruction

All scanning was performed on the ECAT EXACT HR+ scanner in 3D mode (Siemens/CTI, Knoxville, TN). [^{18}F]fallypride was injected i.v. over 30 s. Emission data were acquired over 240 min in 3 successive blocks: 50 min of emission data, followed by a 10 min transmission scan for attenuation correction, followed by a 20 min break, 60 min emission

scan, 10 min transmission scan, 40 min break, 10 min transmission scan and finally a 40 min emission scan. In the first 50 min block, data were acquired as frames of increasing duration (3 * 20 s, 3 * 1 min, 3 * 2 min, 2 * 5 min, 3 * 10 min). In the subsequent 60 and 40 min blocks, all data were binned into 10 min frames. After attenuation correction, data were reconstructed by filtered backprojection with a Shepp filter (cutoff 0.5 cycles/projection ray).

Arterial Input

Following radiotracer injection, arterial samples were collected to form an input function for kinetic modeling. Samples were collected every 10 s with an automated sampling system for the first two min, and manually thereafter at longer intervals. A total of 32 samples were obtained per scan. Following centrifugation (10 min at 1,800 g), plasma was collected in 200 μL aliquots and activities were counted in a gamma counter (Wallac 1480 Wizard 3M Automatic Gamma Counter). Five samples (collected at 2, 20, 40, 80 and 120 min) were further processed by high pressure liquid chromatography (HPLC) to measure the fraction of plasma activity representing unmetabolized parent compound. The unmetabolized parent fraction was fitted to a sum of 2 exponential functions with the smaller exponential rate constant constrained to the difference between the terminal rate of the total plasma activity and the terminal rate in the reference region (cerebellum) (Abi-Dargham et al., 1999). Because of the low signal to noise ratio in plasma samples obtained late in the scan, this method was used to ensure the terminal washout rate of unmetabolized radioligand in arterial plasma was physiologically reasonable. When brain efflux of the radioligand is governed by the concentration gradient across the BBB, the washout rate of radioligand from a reference region asymptotically approaches that of the unmetabolized compound concentration in arterial plasma. As the parent compound concentration is equal to the product of the parent-fraction and the total plasma counts, constraining the parent-fraction terminal rate to the late frame difference between the reference region efflux rate and the total plasma efflux rate ensures that the modeled parent-fraction will be close to the true parent-fraction. The parent-fraction curve was multiplied with the total plasma concentration to obtain an empirical parent-compound curve. The empirical parent-compound curve was then fitted to a sum of 3 exponentials (from the time of peak concentration) and this fitted curve was used as the input function for kinetic modeling. Peripheral clearance (L/hr) of unmetabolized radioligand was computed as the injected activity divided by the total area under the curve of the (decay corrected) modeled plasma input function. Prior to radiotracer injection, a separate sample of arterial plasma was obtained to determine the free fraction (fraction not bound to plasma protein, f_p). Triplicate 200μL aliquots of plasma from blood collected prior to tracer injection were spiked with radiotracer, pipetted into ultrafiltration units (Amicon Centrifree, Millipore, Bedford, MA) and centrifuged at room temperature (20 min at 1,100g). Both plasma and ultrafiltrate actitivities were counted, and f_p was calculated as the ratio of ultrafiltrate activity to total plasma activity concentrations (Gandelman et al., 1994).

Radiochemistry

[^{18}F]fallypride was prepared by reacting the starting material tosylate (2–3 mg) with resolubilized K[^{18}F]F/K222 in acetonitrile (1 ml) at 80° C for 15 min. The starting material was prepared according to a modified literature procedure (Mukherjee et al., 1996). The crude reaction mixture was mixed with water (20 ml) and passed through a C-18 Sep-Pak. The Sep-Pak was washed with 20 ml of 20% aqueous ethanol and the crude product was recovered with 1.5 ml of ethanol, which was then purified by a semipreparative HPLC method (solvent conditions 35% acetonitrile, 65% triethylamine). The HPLC product fraction was mixed with 100 ml of water and passed through a C-18 Sep-Pak. After 20% ethanol (10 ml) and water (10 ml) wash, the tracer was recovered from the Sep-Pak using 1

ml of absolute ethanol. The average radiochemical yield was about 30% at the end of bombardment (EOB) or about 15% at the end of synthesis (EOS). A small sample from the ethanol solution was removed for the determination of specific activity, radiochemical purity and chemical purity. The rest of the ethanol solution was diluted with saline (9 ml) and filtered through a sterile membrane filter into a vented sterile sample vial.

Data preprocessing

PET data were coregistered to each individual's MRI scan. Regions of interest (ROIs) were drawn on the MRIs and transferred to the coregistered PET data. Extrastriatal ROIs incluced amygdala, hippocampus, midbrain/substantia nigra, thalamus, entorhinal cortex, subgenual cortex, uncus, temporal cortex, dorsolateral prefrontal cortex, medial frontal cortex, orbito-frontal cortex, anterior cingulate cortex, parietal cortex and occipital cortex, (see Table II – Table V for abbreviations). A gray matter mask was applied to cortical ROIs so that only gray matter activity was measured in those regions (Abi-Dargham et al., 2000). Striatal ROIs consisted of the limbic striatum, including the ventral striatum (VST), associative striatum (AST) including precommissural dorsal caudate and putamen and post-commissural caudate (Pre-DCA, pre-DPU, and Post-CA) and sensory-motor striatum (Post commissural putamen Post-PU). Additionally, an ROI was applied to globus pallidus (GP). Other than GP, striatal subregions were defined as in (Martinez et al., 2003). The GP was drawn as the region lateral to the internal capsule and medial to putamen on coronal slices posterior to VST and anterior to thalamus (Figure 1). Cerebellum (CER) was also included as a reference region. All other regions were defined as in (Abi-Dargham et al., 2000). Additionally, voxelwise analysis was performed without predefined regions of interest. For these analyses, subjects' MRI scans were normalized into MNI template space in the SPM2 software environment (Friston et al., 1995) and the transformation parameters then applied to coregistered binding maps.

Data analysis and statistics

Data were analyzed by 2-tissue compartment modeling (2TC) with arterial plasma input and by the simplified reference tissue model (SRTM) (Lammertsma and Hume, 1996) using CER as a reference region. For 2TC modeling, total distribution volume (V_T) was estimated in each brain region. CER V_T was taken as an estimate of the nondisplaceable distribution volume (V_{ND}) and was estimated both by 2TC and 1TC models. The small sample Akaike information criterion (AICc) (Burnham and Anderson, 1998) was used to determine which model was more parsimonious in CER. The outcome measures BP_P and BP_{ND} were then determined from regional V_T values according to the formulae:

$$\begin{aligned} BP_P &= V_T(ROI) - V_T(CER) \\ BP_{ND} &= \frac{V_T(ROI)}{V_T(CER)} - 1 \end{aligned} \qquad \text{Eq 1}$$

For SRTM, a basis function approach was used, as this has been demonstrated to be more stable in low binding regions than a conventional gradient based iterative method (Frankle et al., 2006; Gunn et al., 1997). Basis function based SRTM was also used to compute BP_{ND} maps for voxelwise analysis. For each outcome measure, the change following amphetamine (ΔBP) was then computed as

$$\Delta BP = \left(\frac{BP(\text{amphetamine condition})}{BP(\text{baseline})} - 1 \right) \times 100\% \qquad \text{Eq 2}$$

To assess the statistical significance of the amphetamine effect, paired t tests were computed for each region, followed by the false discovery rate adjustment (FDR, Benjamini and Hochberg, 1995) for multiple comparisons, using $\alpha = 0.05$ as the significance threshold. Paired t tests were also used to examine scan parameters (parameters that do not reflect receptor availability) between conditions. Paired t tests implemented in the SPM2 software environment were used to assess amphetamine effect in voxelwise maps. To assess whether there were gender differences in baseline binding or response to amphetamine by gender, repeated measures ANOVA (RMANOVA) with regional BP or ΔBP as repeated measure and gender as between subject variable was performed for each of the 3 outcome measures (2TC BP_{ND}, 2TC BP_P and SRTM BP_{ND}).

Correlation between subjects' amphetamine levels and the relative change in their PET outcome measures (ΔV_T, ΔBP_P, ΔBP_{ND}) were tested with the Pearson product-moment correlation coefficient in each region.

Results

Scan parameters are displayed in Table I. There were no significant changes between conditions in plasma free fraction, nonspecific distribution volume, injected activity, injected mass or specific activity. Following amphetamine there was a small but significant decrease in clearance of unmetabolized [^{18}F] fallypride from arterial plasma ($-11 \pm 19\%$, $p = 0.03$). The AICc scores were significantly lower for the 1TC model than the 2TC in CER ($p = 0.009$, paired t test), indicating the 1TC model was more parsimonious in CER. BP_{ND} results are displayed in Table II for the 2TC model and Table III for the SRTM model. BP_P results are displayed in Table IV. Qualitatively, both BP_{ND} approaches gave similar results, with amphetamine-induced decreases in BP_{ND} in all striatal subregions that tended to be more detectable in the VST and subregions of the putamen than in the subregions of the caudate, as well as detectable decreases in midbrain (SN), amygdala, hippocampus and uncus. The estimated magnitude of the decreases tended to be greater with the 2TC method than the SRTM approach. Significant differences were not readily detected in cortical regions, commensurate with the low baseline BP_{ND} values measured in these regions and resulting low signal to noise ratio. Using the FDR criterion with $\alpha = 0.05$, the 2TC approach for BP_{ND} showed significant decreases in VST, Post-PU, GP, hippocampus and midbrain (SN), whereas only VST and Post-PU reached the FDR criterion for significance with SRTM. For the outcome measure BP_P, decreases following amphetamine were more pronounced, with all high and moderate binding regions exceeding the FDR criterion for significance except the entorhinal cortex. Voxelwise binding maps also showed significant decreases in putamen and ventral striatum after correction for multiple comparisons (Figure 2 and Figure 3). There were no significant differences between genders in baseline binding or amphetamine effects in any of the 3 binding measures.

Plasma amphetamine levels were 77 ± 22, 63 ± 17 and 60 ± 15 ng/ml at 10, 20 and 40 min following amphetamine injection. Peak amphetamine levels and area under the curve (AUC) of amphetamine were highly negatively correlated with ΔBP_P (and ΔV_T) in most regions (except for subregions of the frontal cortex) but not with ΔBP_{ND} obtained with either 2TC or SRTM (Table V).

Discussion

In this study, we used [^{18}F]fallypride to detect the effect of amphetamine challenge in healthy volunteer subjects in striatal and extrastriatal brain regions. Using the outcome measure BP_{ND}, we observed robust effects in the striatum, globus pallidus, midbrain (including substantia nigra) and limbic regions (hippocampus and amygdala), and trend

level effects in thalamus and uncus. We were unable to reliably detect an amphetamine effect in cortical regions such as the DLPFC, orbito-frontal or medial-frontal cortex. This is likely due to the low receptor density and resulting low signal obtained with [^{18}F]fallypride in these regions. While all outcome measures decreased in these regions following amphetamine, the decrease failed to reach statistical significance with either BP_{ND} measure (2TC or SRTM), reflecting the large relative variability of binding potential measurements in cortex with [^{18}F]fallypride. Cortical regions such as DLPFC and orbito-frontal cortex are of particular interest in the study of several psychiatric diseases, but the combination of low baseline values and high variability in ΔBP_{ND} observed in our data suggest that [^{18}F]fallypride is not an optimal tool for examination of cortical D_2 levels or dopaminergic function. [^{11}C] FLB 457 BP_{ND} in cortical regions is in the range of 0.6 to 1, suggesting the possibility that this ligand may provide more reliable results than [^{18}F]fallypride in cortex. Two recently published studies have examined amphetamine effect in cortex with [^{11}C] FLB 457. In one of these (Narendran et al., 2009), [^{11}C] FLB 457 and [^{11}C]fallypride were compared directly in the same subjects. A robust effect of amphetamine was observed in cortex using [^{11}C]FLB 457, but not with [^{11}C]fallypride. In the other study, (Aalto et al., 2009), amphetamine effect was compared to placebo, rather than baseline conditions, using [^{11}C] FLB 457. These authors did not detect an effect of amphetamine compared to placebo. The use of placebo, rather than baseline, as a control condition makes it difficult to compare this interesting study to others in which baseline was the control condition, and while placebo control is an appropriate comparison condition for testing efficacy of therapies, it is not necessarily a more suitable method for finding biomarkers in patient populations than comparison to baseline conditions. Placebo induced alterations in [^{11}C] raclopride binding have been reported in a number of settings: patients with Parkinson's disease in studies of symptom alleviating treatments (apomorphine, de la Fuente-Fernández et al., 2001; trans-cranial magnetic stimulation, Strafella et al., 2006), in healthy subjects anticipating psychostimulant administration (Kaasinen et al., 2004), in healthy subjects anticipating administration of analgesics (Scott et al., 2007) and, in fact, following sensitization, in anticipation of amphetamine (Boileau et al., 2007). For reviews, see (Faria et al., 2008; Oken, 2008). Thus it is not a priori clear that placebo is equivalent to a null condition for cortical dopamine release. True placebo response has the potential to reduce the power to observe true pharmacologically induced effect; it is even conceivable that differences in dopamine storage and release capacity between patients and controls could be confounded rather than clarified by different responses to placebo treatment. On the other hand, a considerable body of imaging data has documented differences in striatal responses to amphetamine relative to baseline conditions in human patient populations compared to control subjects. For example, such studies have been used to examine patients with schizophrenia (Abi-Dargham et al., 1998; Breier et al., 1997; Laruelle et al., 1996) and substance and alcohol abusers (Martinez et al., 2005; Martinez et al., 2007; Munro et al., 2006a). Thus we believe that based on currently available data, comparison to baseline rather than placebo is the appropriate tool for examining cortical dopaminergic function in patient populations with PET.

Table VI presents Spearman rank order coefficients for the amphetamine effect observed with various analyses in this study and comparable regions from other reports. The rank orders were very similar in comparison to (Martinez et al., 2003), moderately similar compared to (Riccardi et al., 2006a), and somewhat dissimilar to those in (Cropley et al., 2008). One possible reason for this observation could be the lack of identity in region definitions. Striatal regions in this study and those from (Martinez et al., 2003) were drawn in the same laboratory by raters with identical training using identical region definitions and software. This was not the case for the other studies. Extra-striatal regions were not identically defined. However, the striatal subregions appearing in Table V of (Cropley et al., 2008) were the same as those used here, and thus this explanation doesn't account for the

low Spearman coefficients in that comparison. Another possible reason for the observed differences is the mode of amphetamine administration (oral vs i.v.). It is reasonable to assume that the profile of amphetamine concentration over time in brain tissue is different between these two methods and this in turn could impact the time profile of dopamine release and the resulting apparent changes in [^{18}F] fallypride specific binding. Amphetamine induces dopamine release through multiple actions including reversal of dopamine transporters, blockade of reuptake through dopamine transporters, reversal of vesicular uptake, blockade of vesicular uptake and inhibition of MAO (Sulzer et al., 2005). Each of these processes has its own concentration dependent kinetics, and each contributes to dopamine release; thus it is plausible that the two modes of administration result in different time profiles of dopamine release, leading to different effects on apparent radioligand binding. Another study in which amphetamine at a dose of 0.3 mg/kg i.v. was administered (Drevets et al., 2001) used somewhat different definitions of brain regions than the current study but nevertheless observed results that were qualitatively similar in terms of overall rank order and magnitude of ΔBP_{ND}. Those authors observed approximately 15% ΔBP_{ND} in subregions containing VST and parts of putamen, and lower (2 to 4%) decreases in subregions containing caudate, in closer agreement with this study and (Martinez et al., 2003) than with (Cropley et al., 2008;Riccardi et al., 2006a), supporting the role of mode of administration on observed amphetamine effect.

While the rank order and mean magnitude of amphetamine effect in striatal subregions in this study were similar to those in (Martinez et al., 2003), the power to detect these effects was not. The left panel of Figure 4 shows a comparison between mean and standard deviations of ΔBP in striatal subregions and several composite regions included in that report and this study. The means are highly correlated (Table VI). However, variability about the mean is larger in this study than in the [^{11}C] raclopride study (right panel, Figure 4). This resulted in smaller effect sizes (mean normalized to standard deviation) for [^{18}F] fallypride displacement compared to [^{11}C] raclopride across all subregions of the striatum (Figure 4). The increased variance of amphetamine effect we observed with [^{18}F] fallypride compared to [^{11}C] raclopride may be related to the difficulty of this study: long scans, multiple attenuation correction maps for each scan, and long duration – several days to several weeks – between baseline and amphetamine condition.

Cerebellum distribution volume

The cerebellar distribution volume (V_{ND}, Table 1) changed little in the mean across conditions but displayed high variance (Δ Cerebellum $V_T \pm SD = -3 \pm 26$ %; the test-retest statistic, equal to absolute change in V_{ND} across conditions divided by average V_{ND} across conditions was 18 ± 15%). The small average change indicates little or no bias, i.e. that there was no detectable effect of amphetamine in the cerebellum. However, the high variability may have contributed to high variability of ΔBP. Cerebellum V_T was low (Table 1) which may have contributed to its poor reproducibility. This quantity enters binding potential measures, either explicitly in the case of plasma-input based methods or implicitly for SRTM, and thus influences their reproducibility. Test-retest variability of V_{ND} was not examined in (Cropley et al., 2008) as arterial plasma was not collected in that study.

Effect of outcome measure

In this study, the regional rank order of ΔBP was the same for all 3 methods of analysis. However ΔBP as measured using BP_P was of greater magnitude and significant in more regions than ΔBP measured with BP_{ND} either using plasma input or the SRTM approach. ΔBP_P was also more correlated with plasma amphetamine levels than the other methods. Both of these results are reflective of the fact that the change in total distribution volumes (ΔV_T) displayed the same properties (data not shown), but correlation with amphetamine

level and magnitude of ΔBP were both reduced when data were normalized to cerebellum distribution volume (V_{ND}) to obtain BP_{ND}. As noted above, V_{ND} itself did not decrease significantly following amphetamine ($\Delta V_{ND} = -3 \pm 26\%$ and Table I, $p = 0.41$), and ΔV_{ND} was not as highly correlated with amphetamine levels as ΔV_T was in most regions; in cerebellum, $R = -0.43$ and $p = 0.14$, whereas ΔV_T correlations with amphetamine were significant or at trend level in all receptor rich regions (data not shown). Intravenous amphetamine administration has been shown to alter regional cerebral blood flow (rcbf) for a period of time following injection (Price et al., 2002) and we have previously demonstrated on theoretical grounds that changing rcbf during the scanning session would lead to artifactual changes in V_T measurements (Slifstein et al., 2004). In this study, the post-amphetamine scans began 30 min after amphetamine injection to minimize rcbf related confounds, but we cannot rule out the possibility that there were some remaining effects that may have been more evident in BP_P than BP_{ND}. In this context it is noteworthy that equilibrium analysis during a steady state of radioligand concentration as in (Martinez et al., 2003) is not vulnerable to fluctuations in rcbf, but this technique is not practical to use with [^{18}F] fallypride, given the long time necessary to reach steady state (Slifstein et al., 2004).

Partial volume effect in limbic regions and GP

In this study, hippocampus, and to a lesser degree amygdala, displayed ΔBP of similar magnitude to striatum. We previously observed a similar effect in anesthetized non-human primates following 1 mg/kg amphetamine and a single bolus scanning protocol with [^{18}F]fallypride (Slifstein et al., 2004, ΔBP = 49% in striatum, 38% in hippocampus, 28% in midbrain and 25% in thalamus). This raises the possibility that the results may have been skewed due to partial volume effect (PVE) contamination from the striatum. However, we have previously presented a model for estimation of artifacts in measured extrastriatal ΔBP due PVE spillover from striatum (Slifstein et al., 2004), showing that PVE has much less influence on ΔBP than on BP itself. The analysis in the appendix shows that ΔBP in hippocampus and amygdala are a weighted sum of ΔBP from these regions plus a small contribution from post-commissural putamen, in the approximate proportions:

$$\Delta BP_{HIP}(apparent) = 88\%\Delta BP_{HIP}(true) + 2\%\Delta BP_{POST-PU}(true) + 10\%\Delta BP_{AMY}(true)$$
$$\Delta BP_{AMY}(apparent) = 5\%\Delta BP_{HIP}(true) + 2\%\Delta BP_{POST-PU}(true) + 93\%\Delta BP_{AMY}(true)$$

indicating that the influence of striatum on ΔBP in these regions is small and in particular that the large change in hippocampus was not a PVE artifact.

Globus Pallidus is in close proximity to several subregions of the striatum, such that PVE effects are more prevalent. However, the analysis in the appendix shows that PVE correction results in nominal reduction of ΔBP in GP from the measured 9% to 8% (Table VII).

Conclusions

Our study shows that while [^{18}F] fallypride allows measurement of the simultaneous effect of amphetamine challenge in striatal subregions and extrastriatally in limbic subregions (hippocampus and amygdala) following a single administration of amphetamine, it fails to do so for cortical regions. Furthermore, the current data set shows a smaller effect size in striatal subregions than data we previously acquired with [^{11}C] raclopride under very similar conditions. In addition, scan durations were 4 hrs, and pre and post challenge studies cannot be performed on the same day. We conclude that greater power might be obtainable with [^{11}C] raclopride for testing hypotheses specific to the striatum. More studies are needed to assess the reliability of the amphetamine effect observed in cortical regions with [^{11}C] FLB

457 (Narendran et al., 2009). If confirmed, this would offer a better alternative to [^{18}F] fallypride to probe dopaminergic transmission in the cortex.

Acknowledgments

The authors wish to acknowledge the excellent technical support in radiochemistry from Dileep Kumar and his staff at the Columbia University radioligand laboratory and in data analysis from Erica Scher and Olga Kambalov. Funding support was provided by NIMH MH0661710-03.

References

Aalto S, Bruck A, Laine M, Nagren K, Rinne JO. Frontal and temporal dopamine release during working memory and attention tasks in healthy humans: a positron emission tomography study using the high-affinity dopamine D-2 receptor ligand [C-11]FLB 457. Journal of Neuroscience. 2005; 25(10):2471–2477. [PubMed: 15758155]

Aalto S, Hirvonen J, Kaasinen V, Hagelberg N, Kajander J, Nagren K, Seppala T, Rinne JO, Scheinin H, Hietala J. The effects of d-amphetamine on extrastriatal dopamine D-2/D-3 receptors: a randomized, double-blind, placebo-controlled PET study with [C-11]FLB 457 in healthy subjects. European Journal of Nuclear Medicine and Molecular Imaging. 2009; 36(3):475–483. [PubMed: 18985345]

Abi-Dargham A, Kegeles LS, Zea-Ponce Y, Mawlawi O, Martinez D, Mitropoulou V, O'Flynn K, Koenigsberg HW, Van Heertum R, Cooper T, Laruelle M, Siever LJ. Striatal amphetamine-induced dopamine release in patients with schizotypal personality disorder studied with single photon emission computed tomography and [123I]iodobenzamide. Biological Psychiatry. 2004; 55(10): 1001–1006. [PubMed: 15121484]

Abi-Dargham A, Martinez D, Mawlawi O, Simpson N, Hwang DR, Slifstein M, Anjilvel S, Pidcock J, Guo NN, Lombardo I, Mann JJ, Van Heertum R, Foged C, Halldin C, Laruelle M. Measurement of striatal and extrastriatal dopamine D-1 receptor binding potential with [C-11]NNC 112 in humans: Validation and reproducibility. J Cerebr Blood F Met. 2000; 20(2):225–243.

Abi-Dargham A, Simpson N, Kegeles L, Parsey R, Hwang DR, Anjilvel S, Zea-Ponce Y, Lombardo I, Van Heertum R, Mann JJ, Foged C, Halldin C, Laruelle M. PET studies of binding competition between endogenous dopamine and the D1 radiotracer [11C]NNC 756. Synapse. 1999; 32(2):93–109. [PubMed: 10231129]

Abi-Dargham A, van Dyck C, Kegeles L, Zea-Ponce Y, Baldwin R, Innis R, Laruelle M. Relationship between amphetamine-induced dopamine release and subjective activation in healthy subjects never previously exposed to psychostimulants. Am J Psych. 1998

Benjamini Y, Hochberg Y. Controlling the False Discovery Rate - A Practical and Powerful Approach to Multiple Testing. Journal of the Royal Statistical Society Series B-Methodological. 1995; 57(1): 289–300.

Boileau I, Dagher A, Leyton M, Welfeld K, Booij L, Diksic M, Benkelfat C. Conditioned dopamine release in humans: A positron emission tomography [C-11] raclopride study with amphetamine. Journal of Neuroscience. 2007; 27(15):3998–4003. [PubMed: 17428975]

Breier A, Su TP, Saunders R, Carson RE, Kolachana BS, deBartolomeis A, Weinberger DR, Weisenfeld N, Malhotra AK, Eckelman WC, Pickar D. Schizophrenia is associated with elevated amphetamine-induced synaptic dopamine concentrations: Evidence from a novel positron emission tomography method. Proc Natl Acad Sci USA. 1997; 94(6):2569–2574. [PubMed: 9122236]

Burnham, K.; Anderson, D. Model selection and inference: a practical information theoretic approach. New York: Springer; 1998. 353 p.

Christian BT, Lehrer DS, Shi BZ, Narayanan TK, Strohmeyer PS, Buchsbaum MS, Mantil JC. Measuring dopamine neuromodulation in the thalamus: Using [F-18]fallypride PET to study dopamine release during a spatial attention task. Neuroimage. 2006; 31(1):139–152. [PubMed: 16469510]

Cropley VL, Innis RB, Nathan PJ, Brown AK, Sangare JL, Lerner A, Ryu YH, Sprague KE, Pike VW, Fujita M. Small effect of dopamine release and no effect of dopamine depletion on [F-18]fallypride binding in healthy humans. Synapse. 2008; 62(6):399–408. [PubMed: 18361438]

Dannals RF, Burns HD, Ravert HT, Langstrom B, Duelfer T, Wilson AA, Zemyan SE, Wagner HN. Radiosynthesis of a Dopamine Receptorbinding Radiotracer for Positron Emission Tomography - [C-11 Methyl]-3-N-Methylspiperone. J Label Compd Radiopharm. 1984; 21(11-1):1146–1147.

de la Fuente-Fernández R, Ruth TJ, Sossi V, Schulzer M, Calne DB, Stoessl AJ. Expectation and dopamine release: mechanism of the placebo effect in Parkinson's disease. Science. 2001; 293(5532):164–1166.

Drevets WC, Gautier C, Price JC, Kupfer DJ, Kinahan PE, Grace AA, Price JL, Mathis CA. Amphetamine-induced dopamine release in human ventral striatum correlates with euphoria. Biological Psychiatry. 2001; 49(2):81–96. [PubMed: 11164755]

Ehrin E, Farde L, de Paulis T, Eriksson L, Greitz T, Johnstrom P, Litton JE, Nilsson JL, Sedvall G, Stone-Elander S, et al. Preparation of 11C-labelled Raclopride, a new potent dopamine receptor antagonist: preliminary PET studies of cerebral dopamine receptors in the monkey. Int J Appl Radiat Isot. 1985; 36(4):269–273. [PubMed: 3874833]

Farde L, Suhara T, Nyberg S, Karlsson P, Nakashima Y, Hietala J, Halldin C. A PET study of [C-11]FLB 457 binding to extrastriatal D-2-dopamine receptors in healthy subjects and antipsychotic drug-treated patients. Psychopharmacology. 1997; 133(4):396–404. [PubMed: 9372541]

Faria V, Fredrikson M, Furmark T. Imaging the placebo response: a neurofunctional review. European Neuropsychopharmacology. 2008; 18:473–485. [PubMed: 18495442]

Finnema SJ, Seneca N, Farde L, Shchukin E, Sovago J, Gulyas B, Wikstrom HV, Innis RB, Neumeyer JL, Halldin C. A preliminary PET evaluation of the new dopamine D-2 receptor agonist [C-11]MNPA in cynomolgus monkey. Nuclear Medicine and Biology. 2005; 32(4):353–360. [PubMed: 15878504]

Frankle WG, Slifstein M, Gunn RN, Huang Y, Hwang DR, Darr EA, Narendran R, Abi-Dargham A, Laruelle M. Estimation of serotonin transporter parameters with C-11-DASB in healthy humans: Reproducibility and comparison of methods. Journal of Nuclear Medicine. 2006; 47(5):815–826. [PubMed: 16644752]

Friston KJ, Holmes AP, Worsley KJ, Poline J-P, Frith CD, Frakowiak RSJ. Statistical parametric maps in functional imaging: A general linear approach. Hum Brain Mapping. 1995; 2:189–210.

Gandelman MS, Baldwin RM, Zoghbi SS, Zea-Ponce Y, Innis RB. Evaluation of ultrafiltration for the free fraction determination of single photon emission computerized tomography (SPECT) radiotracers: β-CIT, IBF and iomazenil. J Pharmaceutical Sci. 1994; 83:1014–1019.

Gunn RN, Lammertsma AA, Hume SP, Cunningham VJ. Parametric imaging of ligand-receptor binding in PET using a simplified reference region model. Neuroimage. 1997; 6(4):279–2787. [PubMed: 9417971]

Hwang DR, Kegeles LS, Laruelle M. (-)-N-[C-11]propyl-norapomorphine: A positron-labeled dopamine agonist for PET imaging of D-2 receptors. Nuclear Medicine and Biology. 2000; 27(6): 533–539. [PubMed: 11056366]

Kaasinen V, Aalto S, Nagren K, Rinne JO. Expectation of caffeine induces dopaminergic responses in humans. European Journal of Neuroscience. 2004; 19(8):2352–2356. [PubMed: 15090062]

Kung HF, Pan S, Kung M-P, Billings J, Kasliwal R, Reilley J, Alavi A. In vitro and in vivo evaluation of [^{123}I]IBZM: a potential CNS D-2 dopamine receptor imaging agent. J Nucl Med. 1989; 30(1): 88–92. [PubMed: 2783457]

Lammertsma AA, Hume SP. Simplified reference tissue model for PET receptor studies. Neuroimage. 1996; 4(3 Pt 1):153–158. [PubMed: 9345505]

Laruelle M, Abi-Dargham A, Gil R, Kegeles L, Innis R. Increased dopamine transmission in schizophrenia: Relationship to illness phases. Biological Psychiatry. 1999; 46(1):56–72. [PubMed: 10394474]

Laruelle M, Abi-Dargham A, van Dyck CH, Gil R, De Souza CD, Erdos J, Mc Cance E, Rosenblatt W, Fingado C, Zoghbi SS, Baldwin RM, Seibyl JP, Krystal JH, Charney DS, Innis RB. Single photon emission computerized tomography imaging of amphetamine-induced dopamine release in drug free schizophrenic subjects. Proc Natl Acad Sci USA. 1996; 93:9235–9240. [PubMed: 8799184]

Laruelle M, Abi-Dargham A, van Dyck CH, Rosenblatt W, Zea-Ponce Y, Zoghbi SS, Baldwin RM, Charney DS, Hoffer PB, Kung HF, Innis RB. SPECT imaging of striatal dopamine release after amphetamine challenge. J Nucl Med. 1995; 36:1182–1190. [PubMed: 7790942]

Laruelle M, Slifstein M, Huang Y. Relationships between radiotracer properties and image quality in molecular imaging of the brain with positron emission tomography. Mol Imaging Biol. 2003; 5(6): 363–375. [PubMed: 14667491]

Mach RH, Nader MA, Ehrenkaufer RLE, Line SW, Smith CR, Luedtke RR, Kung MP, Kung HF, Lyons D, Morton TE. Comparison of two fluorine-18 labeled benzamide derivatives that bind reversibly to dopamine D2 receptors: In vitro binding studies and position emission tomography. Synapse. 1996; 24(4):322–333. [PubMed: 10638823]

Martinez D, Broft A, Foltin RW, Slifstein M, Hwang DR, Huang YY, Perez A, Frankel WG, Cooper T, Kleber HD, Fischman MW, Laruelle M. Cocaine dependence and D-2 receptor availability in the functional subdivisions of the striatum: Relationship with cocaine-seeking behavior. Neuropsychopharmacology. 2004; 29(6):1190–1202. [PubMed: 15010698]

Martinez D, Gil R, Slifstein M, Hwang DR, Huang YY, Perez A, Kegeles L, Talbot P, Evans S, Krystal J, Laruelle M, Abi-Dargham A. Alcohol dependence is associated with blunted dopamine transmission in the ventral striatum. Biological Psychiatry. 2005; 58(10):779–786. [PubMed: 16018986]

Martinez D, Narendran R, Foltin RW, Slifstein M, Hwang DR, Broft A, Huang YY, Cooper TB, Fischman MW, Kleber HD, Laruelle M. Amphetamine-induced dopamine release: Markedly blunted in cocaine dependence and predictive of the choice to self-administer cocaine. American Journal of Psychiatry. 2007; 164(4):622–629. [PubMed: 17403976]

Martinez D, Slifstein M, Broft A, Mawlawi T, Hwang DR, Huang YY, Cooper T, Kegeles L, Zarahn E, Abi-Dargham A, Haber SN, Laruelle T. Imaging human mesolimbic dopamine transmission with positron emission tomography. Part II: Amphetamine-induced dopamine release in the functional subdivisions of the striatum. J Cerebr Blood F Met. 2003; 23(3):285–300.

Mukherjee J, Yang ZY, Brown T, Roemer J, Cooper M. 18F-desmethoxyfallypride: a fluorine-18 labeled radiotracer with properties similar to carbon-11 raclopride for PET imaging studies of dopamine D2 receptors. Life Sciences. 1996; 59(8):669–678. [PubMed: 8761017]

Munro CA, McCaul ME, Oswald LM, Wong DF, Zhou Y, Brasic J, Kuwabara H, Kumar A, Alexander M, Ye WG, Wand GS. Striatal dopamine release and family history of alcoholism. Alcoholism-Clinical and Experimental Research. 2006a; 30(7):1143–1151.

Munro CA, McCaul ME, Wong DF, Oswald LM, Zhou Y, Brasic J, Kuwabara H, Kumar A, Alexander M, Ye WG, Wand GS. Sex differences in striatal dopamine release in healthy adults. Biological Psychiatry. 2006b; 59(10):966–974. [PubMed: 16616726]

Narendran R, Frankel WG, Mason NS, Rabiner E, Gunn RN, Searle GE, Vora S, Litschge M, Kendro S, Cooper T, Mathis C, Laruelle L. Positron emission tomography imaging of amphetamine-induced dopamine release in the human cortex: a comparative evaluation of the high affinity dopamine D2/3 radiotracers [11C]FLB 457 and [11C]fallypride. Synapse. 2009; 63(6):447–461. [PubMed: 19217025]

Narendran R, Hwang DR, Slifstein M, Talbot PS, Erritzoe D, Huang YY, Cooper TB, Martinez D, Kegeles LS, Abi-Dargham A, Laruelle M. In vivo vulnerability to competition by endogenous dopamine: Comparison of the D-2 receptor agonist radiotracer (-)-N-[C-11]propyl-norapomorphine ([I-11]NPA) with the D-2 receptor antagonist radiotracer [C-11]-raclopride. Synapse. 2004; 52(3):188–208. [PubMed: 15065219]

Oken BS. Placebo effects: clinical aspects and neurobiology. Brain. 2008; 131:2812–2823. [PubMed: 18567924]

Oswald LM, Wong DF, McCaul M, Zhou Y, Kuwabara H, Choi L, Brasic J, Wand GS. Relationships among ventral striatal dopamine release, cortisol secretion, and subjective responses to amphetamine. Neuropsychopharmacol. 2005; 30(4):821–832.

Oswald LM, Wong DF, Zhou Y, Kumar A, Brasic J, Alexander M, Ye WG, Kuwabara H, Hilton J, Wand GS. Impulsivity and chronic stress are associated with amphetamine-induced striatal dopamine release. Neuroimage. 2007; 36(1):153–166. [PubMed: 17433881]

Price JC, Drevets WC, Ruszkiewicz J, Greer PJ, Villemagne VL, Xu L, Mazumdar S, Cantwell MN, Mathis CA. Sequential (H2OPET)-O-15 studies in baboons: Before and after amphetamine. Journal of Nuclear Medicine. 2002; 43(8):1090–1100. [PubMed: 12163636]

Riccardi P, Li R, Ansari MS, Zald D, Park S, Dawant B, Anderson S, Doop M, Woodward N, Schoenberg E, Schmidt D, Baldwin R, Kessler R. Amphetamine-induced displacement of [F-18] fallypride in striatum and extrastriatal regions in humans. Neuropsychopharmacology. 2006a; 31(5):1016–1026. [PubMed: 16237395]

Riccardi P, Zald D, Li R, Park S, Ansari MS, Dawant B, Anderson S, Woodward N, Schmidt D, Baldwin R, Kessler R. Sex differences in amphetamine-induced displacement of [F-18] fallypride in striatal and extrastriatal regions: A PET study. American Journal of Psychiatry. 2006b; 163(9): 1639–1641. [PubMed: 16946193]

Rousset OG, Ma Y, Evans AC. Correction for partial volume effects in PET: principle and validation. J Nucl Med. 1998; 39(5):904–911. [PubMed: 9591599]

Scott DJ, Stohler CS, Egnatuk CM, Wang H, Koeppe RA, Zubieta JK. Individual differences in reward responding explain placebo-induced expectations and effects. Neuron. 2007; 55(2):325–336. [PubMed: 17640532]

Slifstein M, Narendran R, Hwang DR, Sudo Y, Talbot PS, Huang YY, Laruelle M. Effect of amphetamine on [F-18]fallypride in vivo binding to D-2 receptors in striatal and extrastriatal regions of the primate brain: Single bolus and bolus plus constant infusion studies. Synapse. 2004; 54(1):46–63. [PubMed: 15300884]

Strafella AP, Ko JH, Monchi O. Therapeutic applicationof transcranial magnetic stimulation in Parkinson's disease: the contribution of expectation. Neuroimage. 2006; 31(4):1666–1672. [PubMed: 16545582]

Sulzer D, Sonders MS, Poulsen NW, Galli A. Mechanisms of neurotransmitter release by amphetamines: A review. Prog Neurobiol. 2005; 75(6):406–433. [PubMed: 15955613]

Volkow ND, Wang G-J, Fowler JS, Logan J, Schlyer D, Hitzemann R, Lieberman J, Angrist B, Pappas N, MacGregor R, Burr G, Cooper T, Wolf AP. Imaging endogenous dopamine competition with [^{11}C]raclopride in the human brain. Synapse. 1994; 16:255–262. [PubMed: 8059335]

Wand GS, Oswald LM, McCaul ME, Wong DF, Johnson E, Zhou Y, Kuwabara H, Kumar A. Association of amphetamine-induced striatal dopamine release and cortisol responses to psychological stress. Neuropsychopharmacol. 2007; 32(11):2310–2320.

Willeit M, Ginovart N, Graff A, Rusjan P, Vitcu I, Houle S, Seeman P, Wilson AA, Kapur S. First human evidence of d-amphetamine induced displacement of a D-2/3 agonist radioligand: A [C-11]-(+)-PHNO positron emission tomography study. Neuropsychopharmacology. 2008; 33(2): 279–289. [PubMed: 17406650]

Wilson AA, McCormick P, Kapur S, Willeit M, Garcia A, Hussey D, Houle S, Seeman P, Ginovart N. Radiosynthesis and evaluation of [11C]-(+)-4-propyl-3,4,4a,5,6,10b-hexahydro-2H-naphtho[1,2-b][1,4]oxazin -9-ol as a potential radiotracer for in vivo Imaging of the dopamine D2 high-affinity state with positron emission tomography. Journal of Medicinal Chemistry. 2005; 48(12):4153–4160. [PubMed: 15943487]

Appendix: Influence of partial volume effect on ΔBP

In its simplest form (contamination of a single region by striatum) the model equation in (Slifstein et al., 2004) is

$$\Delta BP_{ROI}(apparent) = \frac{\frac{w_{ROI,ROI}}{w_{ROI,STR}}\Delta BP_{ROI}(true) + \frac{B_{avail,STR}}{B_{avail,ROI}}\Delta BP_{STR}(true)}{\frac{w_{ROI,ROI}}{w_{ROI,STR}} + \frac{B_{avail,STR}}{B_{avail,ROI}}} \quad \text{Eq 3}$$

where the wij represent geometric spill in from region j to region i (Rousset et al., 1998), i.e. the fraction of observed activity in region i originating in region j if all regions had equal activity. B_{avail} is the concentration of receptors available for binding to [^{18}F] fallypride,

assuming similar affinity across regions. The equation shows that the true ΔBPs in the extrastriatal regions are weighted by the ratio of the geometric factors, whereas the ΔBP in striatum is weighted by the ratio of receptors available for binding in striatum to that in the extrastriatal region. The latter ratio is large, but the former is always larger, so that the observed ΔBP is much closer to true value in the region than to ΔBP of the striatum. A generalization of Eq 3 to include contributions from multiple regions is

$$\Delta BP_i(apparent) = \frac{\alpha_i \Delta BP_i + \sum_{j \neq 1} \alpha_j \Delta BP_j}{\sum_{all\ regions} \alpha_j} \quad \text{Eq 4}$$

where α is defined as

$$\alpha_j = \frac{w_{ij}}{\left(\sum_{k \neq i} w_{ik}\right)} \frac{B_{avail,j}}{B_{avail,i}} \quad \text{Eq 5}$$

The application of Eq 4 requires knowledge of the geometric transfer matrix [wij] as well as the ratios of receptor densities. To estimate the extent of PVE influence on ΔBP in the present data set, we computed the wij for all 15 subjects and averaged laterally and across subjects. From this, it was apparent that the only striatal subregion making non-trivial contributions to hippocampus or amygdala was the Post-PU, although contribution from Post-PU was still small. To estimate B_{avail} ratios, the average GTM was applied to the average (across subjects) baseline V_T, and average PVE corrected BP_{ND} was estimated, yielding the relative values of Post-PU:hippocampus = 21.5, amygdala:hippocampus = 1.8. When Eq.4 is applied using these values the results are

$$\begin{aligned} \Delta BP_{HIP}(apparent) &= 88\%\Delta BP_{HIP}(true) + 2\%\Delta BP_{POST-PU}(true) + 10\%\Delta BP_{AMY}(true) \\ \Delta BP_{AMY}(apparent) &= 5\%\Delta BP_{HIP}(true) + 2\%\Delta BP_{POST-PU}(true) + 93\%\Delta BP_{AMY}(true) \end{aligned}$$

This analysis suggests that PVE contamination from striatum does not explain the large change observed in hippocampus.

In GP, the influence of both subdivisions of the putamen on ΔBP due to PVE is larger than in the case of the hippocampus, due to closer spatial proximity. In this case, all striatal subregions and GP have some PVE influence on each other (i.e. non-zero GTM coefficients) and negligible contributions from extrastriatal regions. The equivalent expression as above for GP is

$$\Delta BP_{GP}(apparent) = 65\%\Delta BP_{GP}(true) + 11\%\Delta BP_{Pre-DPU} + 20\%\Delta BP_{Post-PU} + 4\%\Delta BP_{VST}$$

However, even with the larger contribution from neighboring regions, estimated ΔBP in GP is still quite accurate. When caudate subregions, which make nonzero contributions to putamen and VST but not GP, are included and the system above is inverted, estimated true ΔBP in GP is only reduced from 9 to 8% (Table VII). Thus the principle that PVE is much less influential on ΔBP_{ND} than on BP_{ND} itself is borne out with these data and analyses.

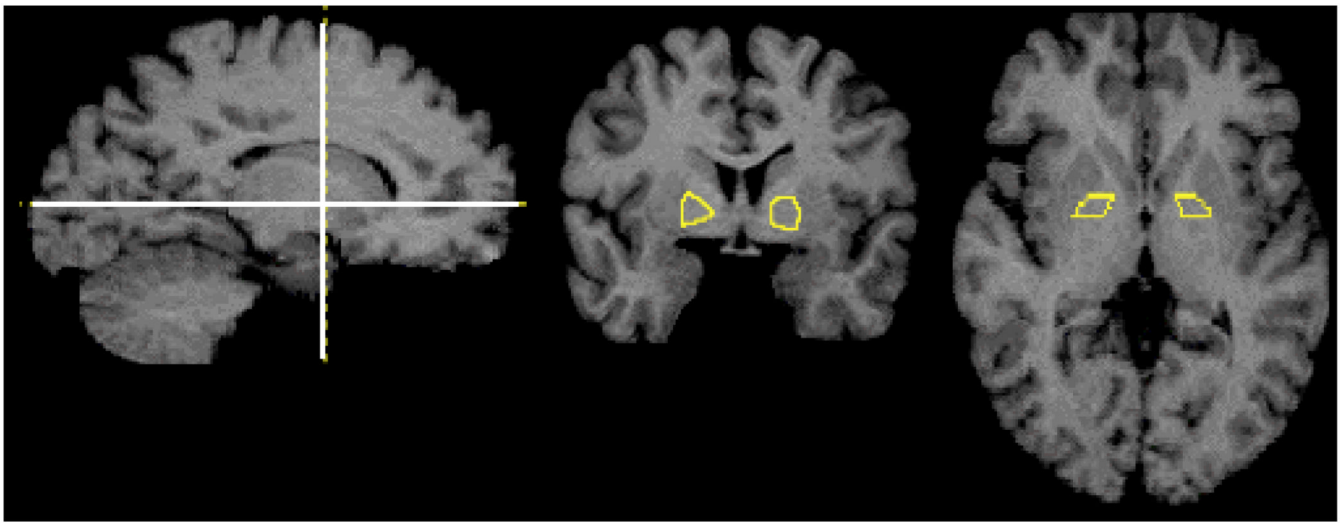

Figure 1.
Globus Pallidus ROI as drawn on one subject's MRI. Lines in the sagittal slice (left) show slice levels of coronal (center) and transverse (right) slices.

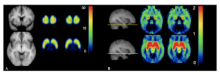

Figure 2.
BP_{ND} maps from SRTM pre and post amphetamine. A At the level of the striatum showing MRI (left), baseline (center) and post-amphetamin (right) in coronal (top) and tranverse (bottom) views. B. Extrastriatal, showing MRI (left) with line at the level of the tranverse slices at baseline (center) and post-amphetamine (right), at the level of the amygdala and temporal cortex (top) and midbrain nuclei (substantia nigra and superior colliculi, bottom). Note the truncated color scale in B, such that all BP_{ND} exceeding 2, including the striatum pre and post amphetamine, appear in red.

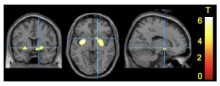

Figure 3.
T maps of amphetamine effect from voxelwise analysis. Following SPM Gaussian random field based correction for multiple comparisons, statistically significant clusters were detected in putamen and ventral striatum only. The display threshold is set at $p < 0.001$.

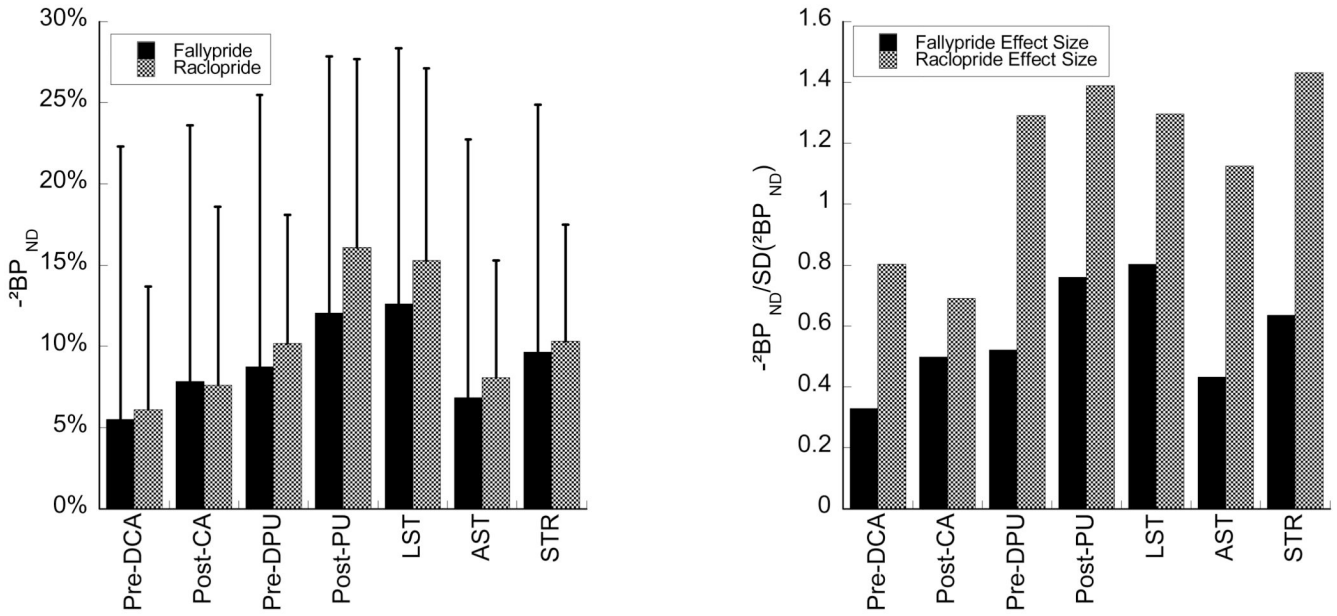

Figure 4.

Comparison [^{11}C] raclopride results to (Martinez et al., 2003). Mean [^{18}F] fallypride regional decreases following amphetamine were of nearly identical magnitude (left) but the between subject variability was higher with the [^{18}F] fallypride paradigm. This is reflected in the effect sizes (mean/SD) of the decrease following amphetamine (right). Region designations are as in Martinez et al. LST (Limbic striatum) is equivalent to the VST. AST (Associative striatum) is a composite of Pre-DCA, Pre-DPU and Post-CA. STR is a composite of all 5 striatal subregions.

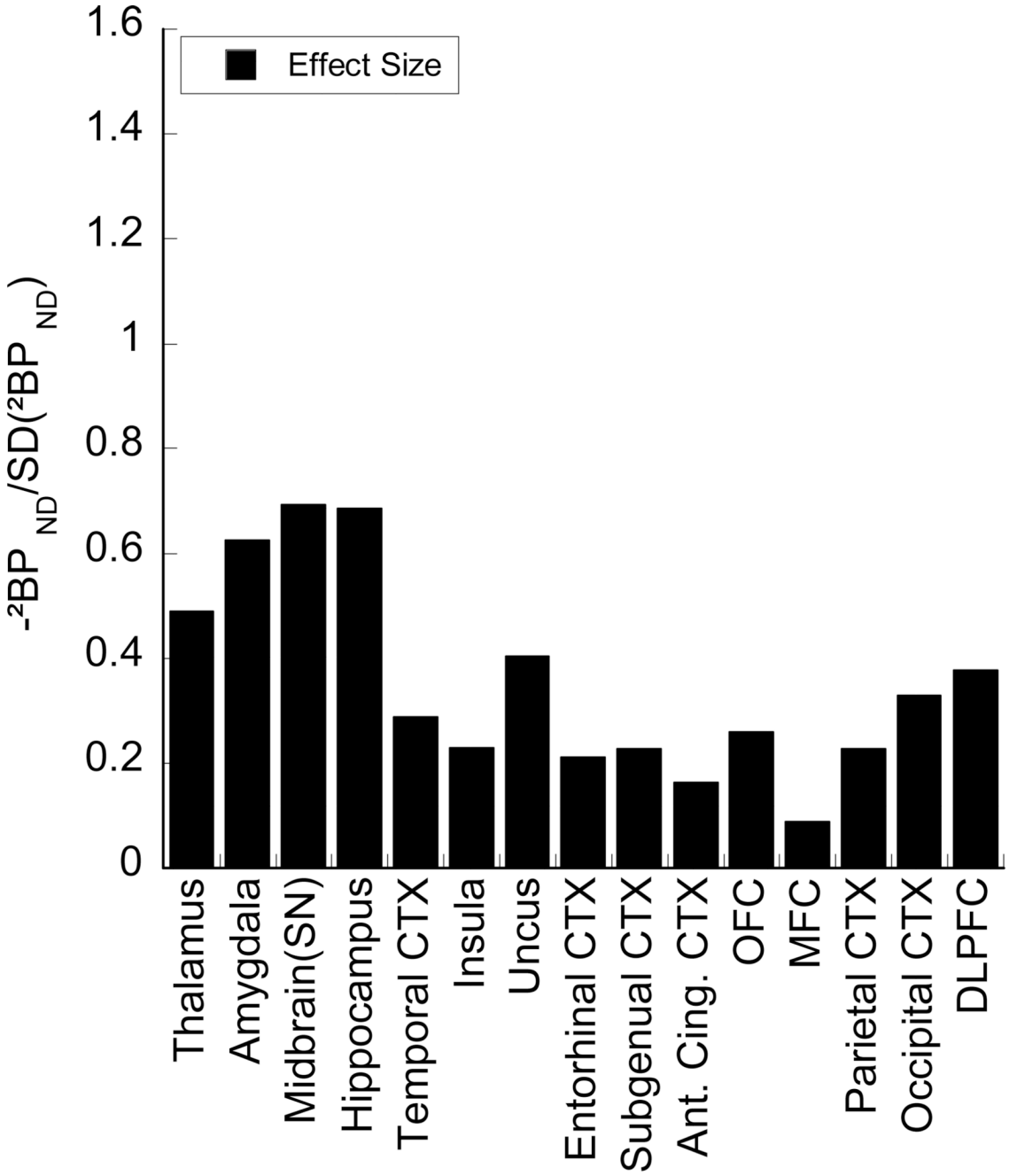

Figure 5.
Effect sizes in extrastriatal regions, displayed on the same scale as the striatal subregions.

Table 1

Scan Parameters

	fp	V_{ND}	ID (mCi)	IM (μg)	SA (Ci/mmol)	CL
Baseline	0.07 ± 0.02	0.70 ± 0.18	3.07 ± 0.90	1.04 ± 0.18	1179 ± 626	18.4 ± 4.3 4.±4.3
Post-Amph	0.07 ± 0.02	0.66 ± 0.18	2.83 ± 1.03	1.03 ± 0.15	1065 ± 592	16.2 ± 3.7
t test (p)	0.72	0.41	0.27	0.97	0.49	0.03

Table II

BP_{ND} (2TC) Amphetamine effect

Bmax		Region	Baseline	Post-Challenge	ΔBP_{ND} (2TC)	Paired t test (p)
High	SMST	Post-PU	23.13 ± 3.57	20.11 ± 3.92	−12 ± 16 %	0.01
	LST	VST	17.93 ± 3	15.48 ± 2.67	−13 ± 16 %	0.01
	AST	Pre-DPU	21 ± 3.04	19.01 ± 3.65	−9 ± 17 %	0.06
		Pre-DCA	17.77 ± 2.64	16.59 ± 2.81	−6 ± 17 %	0.18
		Post-CA	13.15 ± 2.14	12.11 ± 2.57	−7 ± 16 %	0.1
		AST	17.86 ± 2.54	16.5 ± 2.82	−7 ± 16 %	0.12
		Globus Pallidus	11.62 ± 2.03	10.6 ± 2.34	−9 ± 14 %	0.02
Moderate		Thalamus	2.08 ± 0.3	1.94 ± 0.33	−6 ± 13 %	0.06
		Amygdala	1.96 ± 0.4	1.74 ± 0.36	−10 ± 16 %	0.02
		Midbrain(SN)	1.28 ± 0.21	1.15 ± 0.24	−10 ± 15 %	0.01
		Hippocampus	1.08 ± 0.24	0.91 ± 0.26	−15 ± 22 %	0.01
		Temporal CTX	0.84 ± 0.24	0.78 ± 0.24	−6 ± 22 %	0.13
		Insula	1.45 ± 0.36	1.36 ± 0.39	−5 ± 24 %	0.33
		Uncus	1.03 ± 0.29	0.91 ± 0.23	−9 ± 22 %	0.06
		Entorhinal CTX	0.69 ± 0.22	0.64 ± 0.22	−6 ± 29 %	0.21
		Subgenual CTX	0.52 ± 0.18	0.47 ± 0.19	−8 ± 34 %	0.19
Low		Ant. Cing. CTX	0.46 ± 0.11	0.43 ± 0.19	−6 ± 37 %	0.5
		OFC	0.44 ± 0.22	0.37 ± 0.17	−11 ± 41 %	0.13
		MFC	0.39 ± 0.13	0.38 ± 0.17	−4 ± 44 %	0.79
		Parietal CTX	0.38 ± 0.22	0.36 ± 0.25	−44 ± 190 %	0.46
		Occipital CTX	0.31 ± 0.18	0.25 ± 0.2	−42 ± 125 %	0.07
		DLPFC	0.29 ± 0.18	0.28 ± 0.16	−62 ± 164 %	0.6

Table III

BP_{ND} (SRTM) Amphetamine Effect

Bmax		Region	Baseline	Post-Challenge	ΔBP_{ND} (SRTM)	Paired t test (p)
High	SMST	Post-PU	19.49 ± 2.28	17.57 ± 2.17	−10 ± 8 %	< 0.01
	LST	VST	15.17 ± 1.97	13.75 ± 2	−9 ± 9 %	< 0.01
	AST	Pre-DPU	17.79 ± 1.92	16.72 ± 2.05	−6 ± 9 %	0.02
		Pre-DCA	15.04 ± 1.63	14.61 ± 1.87	−3 ± 10 %	0.26
		Post-CA	11.27 ± 2.12	10.76 ± 2.03	−4 ± 13 %	0.21
		AST	15.21 ± 1.64	14.51 ± 1.8	−4 ± 8 %	0.04
		Globus Pallidus	9.88 ± 1.6	9.26 ± 1.73	−6 ± 8 %	0.01
Moderate		Thalamus	1.82 ± 0.21	1.74 ± 0.24	−4 ± 12 %	0.16
		Amygdala	1.71 ± 0.32	1.58 ± 0.29	−7 ± 12 %	0.03
		Midbrain(SN)	1.12 ± 0.17	1.03 ± 0.18	−8 ± 13 %	0.04
		Hippocampus	0.97 ± 0.21	0.88 ± 0.22	−8 ± 18 %	0.1
		Temporal CTX	0.74 ± 0.19	0.7 ± 0.2	−5 ± 19 %	0.19
		Insula	1.29 ± 0.26	1.25 ± 0.27	−3 ± 14 %	0.38
		Uncus	0.9 ± 0.2	0.83 ± 0.18	−6 ± 15 %	0.05
		Entorhinal CTX	0.61 ± 0.17	0.58 ± 0.19	−5 ± 20 %	0.31
		Subgenual CTX	0.47 ± 0.17	0.43 ± 0.14	−5 ± 24 %	0.18
Low		Ant. Cing. CTX	0.42 ± 0.11	0.39 ± 0.14	−5 ± 28 %	0.36
		OFC	0.4 ± 0.14	0.38 ± 0.13	1 ± 33 %	0.45
		MFC	0.36 ± 0.11	0.35 ± 0.13	−1 ± 29 %	0.63
		Parietal CTX	0.35 ± 0.18	0.34 ± 0.2	−2 ± 41 %	0.59
		Occipital CTX	0.28 ± 0.14	0.25 ± 0.14	−13 ± 25 %	0.04
		DLPFC	0.28 ± 0.12	0.27 ± 0.12	−10 ± 27 %	0.72

Table IV

BP_P (2TC) Amphetamine Effect

Bmax		Region	Baseline	Post-Challenge	ΔBP_p	Paired t test (p)
High	SMST	Post-PU	16.12 ± 4.73	13.26 ± 4.46	−18 ± 13 %	< 0.01
	LST	VST	12.31 ± 3.01	10.02 ± 2.42	−18 ± 15 %	< 0.01
	AST	Pre-DPU	14.51 ± 3.82	12.42 ± 3.81	−14 ± 14 %	< 0.01
		Pre-DCA	12.28 ± 3.28	10.91 ± 3.4	−11 ± 13 %	0.01
		Post-CA	9.3 ± 3.38	8.03 ± 2.98	−12 ± 16 %	0.02
		AST	12.37 ± 3.34	10.85 ± 3.4	−12 ± 13 %	< 0.01
		Globus Pallidus	8.05 ± 2.38	6.97 ± 2.42	−14 ± 16 %	0.01
Moderate		Thalamus	1.44 ± 0.41	1.27 ± 0.38	−11 ± 17 %	0.02
		Amygdala	1.33 ± 0.32	1.12 ± 0.29	−15 ± 16 %	0.01
		Midbrain(SN)	0.89 ± 0.26	0.74 ± 0.22	−15 ± 17 %	0.01
		Hippocampus	0.74 ± 0.21	0.59 ± 0.21	−20 ± 21 %	0.01
		Temporal CTX	0.58 ± 0.2	0.5 ± 0.16	−12 ± 20 %	0.01
		Insula	1.01 ± 0.36	0.88 ± 0.35	−12 ± 17 %	0.01
		Uncus	0.7 ± 0.19	0.59 ± 0.19	−15 ± 21 %	0.01
		Entorhinal CTX	0.47 ± 0.16	0.4 ± 0.17	−13 ± 28 %	0.04
		Subgenual CTX	0.36 ± 0.15	0.3 ± 0.14	−15 ± 31 %	0.04
Low		Ant. Cing. CTX	0.32 ± 0.11	0.27 ± 0.14	−14 ± 41 %	0.12
		OFC	0.3 ± 0.14	0.23 ± 0.13	−20 ± 39 %	0.01
		MFC	0.27 ± 0.11	0.24 ± 0.11	−13 ± 45 %	0.08
		Parietal CTX	0.27 ± 0.17	0.22 ± 0.17	−70 ± 251 %	0.01
		Occipital CTX	0.21 ± 0.13	0.15 ± 0.14	−61 ± 161 %	< 0.01
		DLPFC	0.2 ± 0.12	0.17 ± 0.12	−84 ± 191 %	0.06

Table V

Correlation with peak amphetamine. Correlation coefficients and (p values)

Region	ΔBP_p	ΔBP_{ND} (2TC)	ΔBP_{ND} (SRTM)
Post-PU	−0.78 (0.002)	−0.13 (0.664)	0.31 (0.297)
Pre-DPU	−0.67 (0.012)	−0.06 (0.854)	0.49 (0.093)
VST	−0.70 (0.008)	−0.13 (0.670)	0.30 (0.316)
Pre-DCA	−0.65 (0.016)	0.04 (0.897)	0.47 (0.101)
Post-CA	−0.66 (0.014)	−0.11 (0.722)	0.23 (0.442)
Thalamus	−0.64 (0.018)	−0.09 (0.761)	0.10 (0.753)
Amygdala	−0.72 (0.006)	−0.18 (0.549)	0.02 (0.937)
Midbrain (SN)	−0.59 (0.035)	−0.02 (0.946)	0.14 (0.641)
Hippocampus	−0.65 (0.017)	−0.26 (0.385)	−0.11 (0.725)
Temporal CTX	−0.48 (0.100)	0.04 (0.898)	0.13 (0.669)
Insula	−0.62 (0.025)	−0.07 (0.820)	0.16 (0.600)
Uncus	−0.57 (0.040)	−0.13 (0.667)	0.02 (0.949)
Entorhinal CTX	−0.46 (0.117)	−0.09 (0.778)	0.07 (0.812)
Subgenual CTX	−0.39 (0.185)	−0.11 (0.733)	−0.06 (0.839)
Ant. Cing. CTX	−0.32 (0.290)	−0.05 (0.879)	−0.03 (0.910)
OFC	−0.19 (0.527)	0.04 (0.908)	0.05 (0.877)
MFC	−0.23 (0.445)	0.02 (0.950)	0.04 (0.892)
Parietal CTX	−0.04 (0.899)	0.03 (0.917)	0.25 (0.410)
Occipital CTX	−0.03 (0.934)	0.06 (0.847)	0.43 (0.138)
DLPFC	0.10 (0.755)	0.19 (0.540)	−0.19 (0.538)

Table V1

Comparison of rank order of ΔBP to other publications

Method in this report	Table 3, Martinez et al	Table 1, Riccardi et al	Table IV, Cropley et al	Table V, Cropley et al
2TCM BPND	0.90	0.68	0.58	0.20
SRTM BPND	1.0	0.79	0.20	0.50

Numbers are Spearman rank order coefficients. Regions included from Table 3 in Martinez et al and Table V in Cropley et al are Pre-DCA, Pre-DPU, Post-CA, Post-PU and VST. Regions included from Table 1 in Riccardi et al are caudate, putamen, VST, substantia nigra (midbrain), thalamus, amygdala and temporal cortex. Regions included Table IV in Cropley et al are caudate putamen, thalamus, orbito-frontal cortex, temporal cortex, medial-temporal cortex (hippocampus), and substantia nigra (midbrain). Parentheses indicate closest equivalent from the current data set when exact matches were not available.

Table VII

Effect of PVE correction on observed ΔBP_{ND}

	Pre-DPU	Post-PU	Pre-DCA	Post-CA	VST	GP
uncorrected	−9%	−12%	−6%	−8%	−13%	−9%
PVE corrected	−8%	−12%	−5%	−8%	−15%	−8%